

# RSC Advances



This is an *Accepted Manuscript*, which has been through the Royal Society of Chemistry peer review process and has been accepted for publication.

*Accepted Manuscripts* are published online shortly after acceptance, before technical editing, formatting and proof reading. Using this free service, authors can make their results available to the community, in citable form, before we publish the edited article. This *Accepted Manuscript* will be replaced by the edited, formatted and paginated article as soon as this is available.

You can find more information about *Accepted Manuscripts* in the [Information for Authors](#).

Please note that technical editing may introduce minor changes to the text and/or graphics, which may alter content. The journal's standard [Terms & Conditions](#) and the [Ethical guidelines](#) still apply. In no event shall the Royal Society of Chemistry be held responsible for any errors or omissions in this *Accepted Manuscript* or any consequences arising from the use of any information it contains.

**Non-classical CH $\cdots$ O hydrogen-bond determining the regio- and stereoselectivity in the [3+2] cycloaddition reaction of (Z) C-phenyl-N-methylnitrone with dimethyl 2-benzylidenecyclopropane-1,1-dicarboxylate. A topological electron-density study**

Abdelmalek Khorief Nacereddine<sup>\*a,b</sup>, Chafia Sobhi<sup>a</sup>, Abdelhafid Djerourou<sup>a</sup>,

Mar Ríos-Gutiérrez<sup>†c</sup>, Luis R. Domingo<sup>c</sup>

<sup>a</sup>Laboratoire de Synthèse et Biocatalyse Organique, Département de Chimie, Faculté des Sciences, Université Badji Mokhtar Annaba, BP 12, 23000 Annaba, Algeria.

<sup>b</sup>Département de Physique et Chimie, Ecole Normale Supérieure d'Enseignement Technologique de Skikda, Azzaba-Skikda, Algeria.

<sup>c</sup>Departamento de Química Orgánica, Universidad de Valencia, Dr. Moliner 50, E-46100 Burjassot, Valencia, Spain.

**Abstract**

The role of the ester groups in the regio- and stereoselectivities of the *zw-type* [3+2] cycloaddition (32CA) reaction of C-phenyl-N-methylnitrone with dimethyl 2-benzylidenecyclopropane-1,1-dicarboxylate (BCPC) has been studied using DFT methods at the MPWB1K/6-31G(d) level. The possible *ortho/meta* regioisomeric channels and the *endo/exo* stereoselective approach modes were explored and characterized. Analysis of the relative energies associated with the different reaction pathways indicates that the presence of the two CO<sub>2</sub>Me groups in the cyclopropane ring has a remarkable effect on selectivities favouring the *ortho/endo* path, in good agreement with the experimental data. Inclusion of solvent effects increases the activation energy and decreases the exothermic character of both 32CA reactions but does not change gas phase selectivities. The electron localisation function (ELF) topological analysis along the most favourable *ortho/endo* path allows explaining the formation of the C–C and O–C through a non-concerted *two-stage one-step* mechanism. A non-covalent interaction (NCI) analysis of the most favourable *ortho/endo* transition state structure reveals that the formation of a non-classical CH $\cdots$ O hydrogen-bond involving the nitrone C–H hydrogen is responsible for the selectivity experimentally found in this non-polar *zw-type* 32CA reaction.

**Keywords:** [3+2] cycloaddition, benzylidenecyclopropane, Selectivity, Mechanism, DFT calculations, ELF topology, NCIs.

---

Corresponding authors. e-mail address:

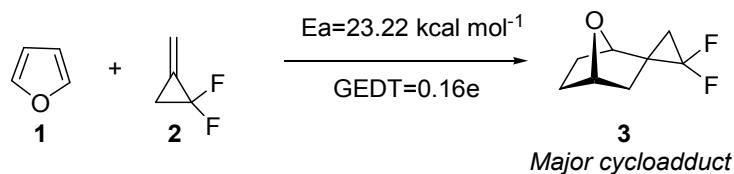
\*khorief.abdelmalek@univ-annaba.org (A.K. Nacereddine).

† m.mar.rios@uv.es (M. Ríos-Gutiérrez)

## 1. Introduction

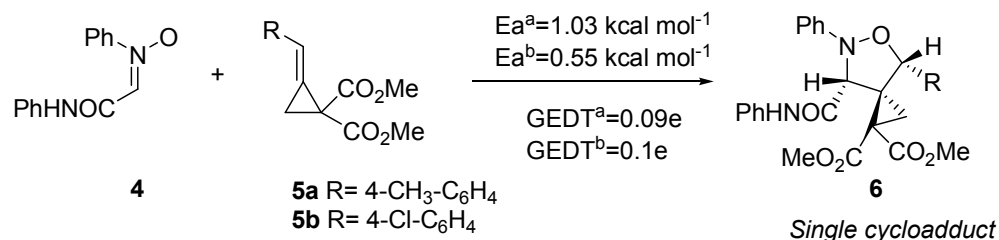
Cycloadditions are among the most useful organic reactions since they enable the preparation of carbocyclic and heterocyclic compounds of great pharmaceutical and industrial interest.<sup>1</sup> [3+2] cycloaddition (32CA) reactions are important processes in organic synthesis and they are widely used to obtain five-membered heterocyclic compounds.<sup>2</sup> Reactions between nitrones and ethylene derivatives leading to isoxazolidines are well-known processes of this kind.<sup>1,2</sup> Substituted isoxazolidines have found numerous applications as enzyme inhibitors<sup>3</sup> and as intermediates for the synthesis of a variety of compounds after cleavage of the N–O bond.<sup>4</sup> On the other hand, the use of methylenecyclopropane derivatives for the synthesis of heterocyclic compounds has widely spread in recent years due to easily accessible methods and their selective synthetic transformations in cycloaddition reactions without the use of catalysts and added reagents.<sup>5</sup>

A considerable amount of experimental and theoretical studies on the mechanisms and selectivities of cycloaddition reactions of methylenecyclopropane derivatives can be found in the literature. Recently, we studied the Diels–Alder reaction between furan **1** and difluoromethylenecyclopropane **2**, finding that the reaction proceeded *via* a synchronous one-step mechanism with high activation energy and a non-polar character (see Scheme 1). This reaction favoured the formation of the *endo* cycloadduct due to the favourable interaction along the *endo* approach mode.<sup>6</sup>



**Scheme 1.** Diels–Alder reaction of furan **1** with difluoro-2-methylenecyclopropane **2**.

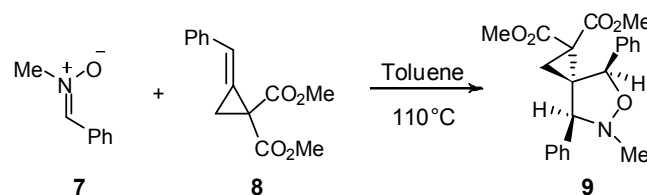
Moeinpour *et al.* studied, using density functional theory (DFT) calculations at the B3LYP/6-31G level, the mechanism and the regioselectivity of the 32CA reaction of *C*-phenyl carbamoyl-*N*-phenylnitron **4** with some dialkyl-substituted 2-benzylidenecyclopropane-1,1-dicarboxylates **5** (see Scheme 2).<sup>7</sup> The authors found that the change of the substituent in the phenyl ring of 2-benzylidenecyclopropane-1,1-dicarboxylates **5** may change the nature of the mechanism for this reaction. They showed that these reactions occur *via* an asynchronous one-step mechanism with non-polar character and low activation energies.



**Scheme 2.** 32CA reaction of *C*-phenyl carbamoyl-*N*-phenylnitrone **4** with dialkyl-substituted 2-benzylidenecyclopropane-1,1-dicarboxylates **5**.

Recently, a useful classification of 32CA reactions into *pseudodiradical-type* (*pr-type*) reactions involving three-atom-components (TACs) with a high *pseudodiradical* character, which take place easily through an earlier transition state structure (TS) with non-polar character, and *zwitterionic-type* (*zw-type*) reactions involving TACs with a high zwitterionic character, controlled by favourable nucleophilic/electrophilic interactions taking place at the TSs, was established.<sup>8</sup> Nitrones, which present a high nucleophilic character, are able to participate in *zw-type* 32CA reactions towards electrophilically activated ethylenes, *via* a polar mechanism with low activation energy.<sup>9</sup>

Tran *et al.* experimentally studied the 32CA reaction between *C*-phenyl-*N*-methylnitrone **7** and dimethyl 2-benzylidenecyclopropane-1,1-dicarboxylate (BCPC) **8**,<sup>10</sup> finding that this reaction is regio- and stereoselective yielding the corresponding *ortho/endo* cycloadduct **9** as the single regio- and stereocycloadduct (see Scheme 3).



**Scheme 3.** 32CA reaction of *C*-phenyl-*N*-methylnitrone **7** with BCPC **8**.

As a continuation of our studies on the selectivities and mechanisms of the 32CA reactions of methylenecyclopropane derivatives,<sup>6</sup> we decided to undertake a theoretical investigation of the regio- and stereoselectivities of the 32CA reaction experimentally performed by Tran's group.<sup>10</sup> In order to explain the role of the ester groups in the reactivity and selectivity of this reaction, the 32CA reactions of *C*-phenyl-*N*-methylnitrone **7** with 2-benzylidenecyclopropane (BCP) **10** and with BCPC **8** were studied.

## 2. Computational Methods

Several works have shown that the B3LYP functional<sup>11</sup> is relatively accurate for kinetic data, although the reaction exothermicities are underestimated.<sup>12</sup> Recently, Truhlar's group proposed some functionals, such as the MPWB1K hybrid meta functional,<sup>13</sup> which improve thermodynamic calculations. Consequently, DFT computations were carried out using the MPWB1K<sup>13</sup> exchange-correlation functional, together with the standard 6-31G(d) basis set.<sup>14</sup> Single point energy calculations at the MPWB1K/6-31+G(d) level were additionally performed in order to test how the diffuse functions modify the selectivities of this 32CA reaction. The stationary points were characterised by frequency computations in order to verify that TSs have one and only one imaginary frequency. Intrinsic reaction coordinate (IRC)<sup>15</sup> pathways were traced to verify the connectivity between minima and associated TSs. Solvent effects of toluene were taken into account through single point energy calculations using the polarisable continuum model (PCM) developed by Tomasi's group in the framework of the self consistent reaction field.<sup>16</sup> Values of enthalpies, entropies and Gibbs free energies in toluene were calculated with standard statistical thermodynamics at 383.15 K and 1 atm over the optimized gas phase structures<sup>17</sup> and were scaled by 0.96.<sup>18</sup>

The electronic structures of critical points were analysed by the natural bond orbital (NBO) method.<sup>19</sup> The electron localisation function (ELF) topological analysis,  $\eta(\mathbf{r})$ ,<sup>20</sup> was performed with the TopMod program<sup>21</sup> using the corresponding MPWB1K/6-311G(d,p) monodeterminantal wavefunctions of the selected structures of the IRC. Non-covalent interactions (NCI) were computed by evaluating the promolecular density and using the methodology previously described.<sup>22,23</sup> All computations were carried out with the Gaussian 09 suite of programs.<sup>24</sup>

The global electrophilicity index  $\omega$ ,<sup>25</sup> which measures the stabilisation in energy when the system acquires an additional electronic charge  $\Delta N$  from the environment, is expressed by the following simple equation,<sup>25</sup>  $\omega = (\mu^2/2\eta)$ , in terms of the electronic chemical potential,  $\mu$ , and the chemical hardness,  $\eta$ . Both quantities may be approached in terms of the one electron energies of the frontier molecular orbitals HOMO and LUMO,  $\epsilon_H$  and  $\epsilon_L$ , as  $\mu \approx (\epsilon_H + \epsilon_L)/2$  and  $\eta = (\epsilon_L - \epsilon_H)$ , respectively.<sup>26</sup> On the other hand, the nucleophilicity index is defined as  $N = \epsilon_{\text{HOMO}} - \epsilon_{\text{HOMO(TCE)}}$ ,<sup>27</sup> where  $\epsilon_{\text{HOMO}}$  is the HOMO energy of the nucleophile and  $\epsilon_{\text{HOMO(TCE)}}$  corresponds to the HOMO energy of tetracyanoethylene (TCE), taken as a reference. The

electrophilic,  $P_k^+$ , and nucleophilic,  $P_k^-$ , Parr functions<sup>28</sup> were obtained through the analysis of the Mulliken atomic spin densities of the corresponding radical anion and radical cation by single-point energy calculations over the optimised neutral geometries.

### 3. Results and discussion

The present study has been divided into six sections: i) first, the 32CA reaction between *C*-phenyl-*N*-methylnitronone **7** and BCP **10** is studied; ii) in the second part, the 32CA reaction between nitronone **7** and BCPC **8** is theoretically investigated. In each part, energetic aspects, geometrical parameters of the TSs and their electronic structures in terms of natural charges are analysed. Solvent effects on these 32CA reactions are also discussed; iii) in the third part, an ELF topological analysis of the formation of the C–C and O–C single bonds along the most favorable *ortho/endo* path associated with the 32CA reaction of nitronone **7** with BCPC **8** is carried out; iv) in the fourth part, the NCIs of the TS involved in the most favourable *ortho/endo* path associated with this 32CA reaction are analysed; v) in the fifth part, a DFT analysis based on the reactivity indices is performed; and finally, vi) in the last part, the origin of the *ortho/endo* selectivity in the 32CA reaction reaction of nitronone **7** with BCPC **8** is explained.

The zwitterionic TAC, nitronone **7**, and BCPC **8** and BCP **10**, are unsymmetrical species, thereby, the interaction TAC/ethylene can take place through four reactive channels corresponding to the *endo* and *exo* stereoisomeric approach modes of BCPC **8** and BCP **10** towards nitronone **7**, and the two regioisomeric modes: the *ortho* and *meta* pathways. Thus, four TSs and four cycloadducts were located for each reaction path (see Scheme 4).

#### 3.1 Study of the 32CA reaction between nitronone **7** and BCP **10**

First, the *zw-type* 32CA reaction between nitronone **7** and BCP **10** was studied (see Scheme 4). The MPWB1K/6-31G(d) total and relative energies are summarized in Table 1. The MPWB1K/6-31G(d) gas phase activation energies associated with the four reactive channels of the 32CA reaction between nitronone **7** and BCP **10** are 16.4 (TS-10-on), 18.9 (TS-10-ox), 14.4 (TS-10-mn) and 15.3 (TS-10-mx) kcal mol<sup>-1</sup>, the reaction being exothermic by between 36 and 40 kcal mol<sup>-1</sup>. This 32CA reaction presents a high activation energy, 14.4 kcal mol<sup>-1</sup> (TS-10-mn). Note that the activation energy associated with the most favourable TS-10-mn is 1.3 kcal mol<sup>-1</sup> higher than that associated with the non-polar 32CA reaction between the simplest nitronone and ethylene.<sup>9</sup> These energy results indicate that this 32CA reaction is

low *endo* stereoselective, as the most favourable *endo* **TS-10-mn** is 0.9 kcal mol<sup>-1</sup> below the *exo* **TS-10-mx**, and displays a moderate *meta* regioselectivity as the most favourable *meta* **TS-10-mn** is 2.0 kcal mol<sup>-1</sup> below the *ortho* **TS-10-on**. Consequently, due to the strong exothermic character of the reaction, which makes the formation of the four CAs irreversible, the differences between the activation energies suggest that this reaction would lead to an isomeric mixture.

**Table 1.** MPWB1K/6-31G(d) total (E, in a.u.) and relative<sup>a</sup> energies ( $\Delta E$ , in kcal mol<sup>-1</sup>) in gas phase and in toluene of the stationary points involved in the 32CA reaction of *C*-phenyl-*N*-methylnitron **7** with BCP **10**.

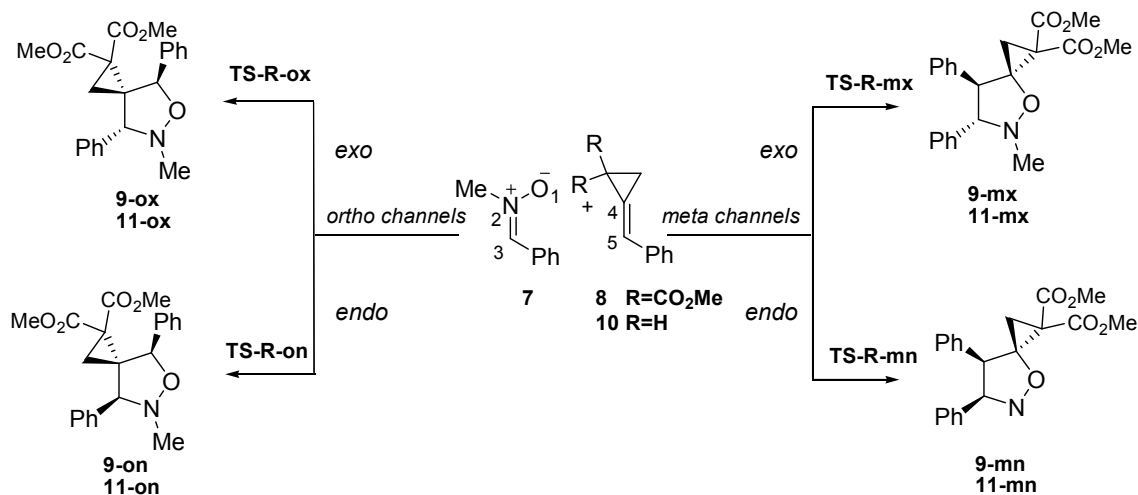
	Gas phase		Toluene	
	E	$\Delta E$	E	$\Delta E$
<b>7</b>	-439.94778		-439.95239	
<b>10</b>	-386.81884		-386.82071	
<b>TS-10-on</b>	-826.74045	16.4	-826.74489	17.7
<b>TS-10-ox</b>	-826.73645	18.9	-826.74091	20.2
<b>TS-10-mn</b>	-826.74359	14.4	-826.74734	16.2
<b>TS-10-mx</b>	-826.74219	15.3	-826.74594	17.0
<b>11-on</b>	-826.82673	-37.7	-826.83014	-35.8
<b>11-ox</b>	-826.83063	-40.2	-826.83387	-38.1
<b>11-mn</b>	-826.82399	-36.0	-826.82766	-34.2
<b>11-mx</b>	-826.82559	-37.0	-826.82927	-35.2

<sup>a</sup> Relative to **7** and **10**.

In order to compare the MPWB1K energy results with the B3LYP ones, the stationary points were optimised at the B3LYP/6-31G(d) level. The B3LYP/6-31G(d) gas phase total and relative energies are given in Table S1 in Supplementary Material. A comparison of the gas phase relative energies indicates that while the B3LYP activation energies are between 3.9 and 5.5 kcal mol<sup>-1</sup> higher than those of the MPWB1K ones, the reaction energies are underestimated by around 18 kcal mol<sup>-1</sup>. Regardless, both functionals yield low selectivity.

Inclusion of solvent effects stabilises all structures in the gas phase calculations; nitron **7** is more stabilised than BCP **10**, TSs and cycloadducts, as a consequence of a higher solvation of nitron **7** than other stationary points in polar solvents.<sup>29</sup> Consequently, solvent effects increase the activation energies by 1.3 kcal mol<sup>-1</sup> for both *ortho* **TS-10-on** and **TS-10-ox**, while for the *meta* TSs they are increased by 1.8 kcal mol<sup>-1</sup> for the *endo* approach and 1.7 kcal mol<sup>-1</sup> for the *exo* one (see Table 1). Thereby, inclusion of solvent effects slightly

increases the activation energies and decreases the exothermic character of this 32CA reaction but does not change the low selectivity obtained in gas phase.



**Scheme 4.** Competitive regio- and stereoisomeric pathways associated with the 32CA reactions of nitron **7** with BCPC **8** or BCP **10**.

The values of the enthalpies, entropies and Gibbs free energies and the relative ones of the stationary points involved in the 32CA reaction of nitron **7** with BCP **10** are summarized in Table 2. The Gibbs free energy profile of the 32CA reaction between nitron **7** and BCP **10** is given in Figure 1. From Table 2, a comparison between the relative activation enthalpies associated with the four reactive pathways of the 32CA reaction of nitron **7** with BCP **10** indicates that the most favourable approach mode is now that associated with **TS-10-mx** ( $\Delta H = 17.6 \text{ kcal mol}^{-1}$ ). Addition of the entropic contribution to the enthalpy increases the activation Gibbs free energy of this reactive channel to  $34.1 \text{ kcal mol}^{-1}$ . However, the analysis of the activation Gibbs free energies indicates that although the *meta/exo* reactive channel becomes the most favourable one as the consequence of the unfavourable negative activation entropy associated with **TS-10-mn**,  $\Delta S = -53.9 \text{ cal mol}^{-1} \text{ K}^{-1}$ , this 32CA reaction shows low selectivity as **TS-10-mx** is only  $0.6 \text{ kcal mol}^{-1}$  more favourable than **TS-10-on**. In addition, this 32CA reaction is exergonic by between  $5.8$  and  $13.3 \text{ kcal mol}^{-1}$ . Consequently, it is expected to obtain an isomeric mixture from this 32CA reaction.

**Table 2.** MPWB1K/6-31G(d) enthalpies (H, in a.u.), entropies (S, in cal mol<sup>-1</sup> K<sup>-1</sup>) and Gibbs free energies (G, in a.u.), and the relative<sup>a</sup> ones ( $\Delta H$  in kcal mol<sup>-1</sup>,  $\Delta S$  in cal mol<sup>-1</sup> K<sup>-1</sup> and  $\Delta G$  in cal mol<sup>-1</sup> K<sup>-1</sup>, respectively), computed at 398.15 K and 1 atm in toluene, for the stationary points involved in the 32CA reaction between nitron 7 and BCP 10.

System	H	$\Delta H$	S	$\Delta S$	G	$\Delta G$
<b>7</b>	-439.78289		103.2		-439.84557	
<b>10</b>	-386.63984		98.6		-386.70004	
<b>TS-10-on</b>	-826.39365	18.2	158.2	-43.6	-826.49027	34.7
<b>TS-10-ox</b>	-826.38981	20.7	156.4	-45.4	-826.48528	37.9
<b>TS-10-mn</b>	-826.39337	18.4	147.9	-53.9	-826.48366	38.9
<b>TS-10-mx</b>	-826.39473	17.6	158.1	-43.7	-826.49122	34.1
<b>11-on</b>	-826.47549	-33.1	149.6	-52.1	-826.56687	-13.3
<b>11-ox</b>	-826.46494	-26.5	155.2	-46.6	-826.56339	-11.2
<b>11-mn</b>	-826.45873	-22.6	151.6	-50.2	-826.55489	-5.8
<b>11-mx</b>	-826.46032	-23.6	154.9	-46.9	-826.55860	-8.1

<sup>a</sup> Relative to 7 and 10.

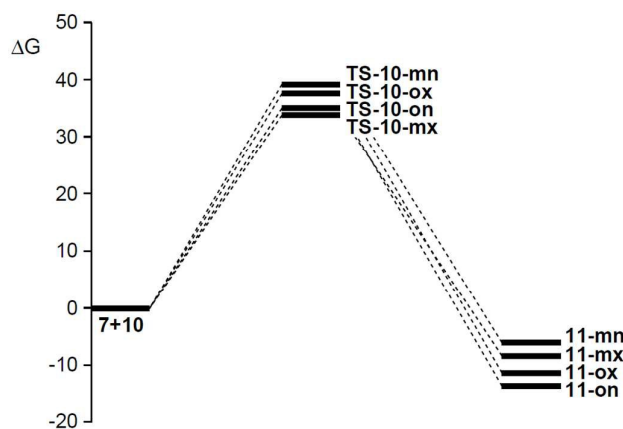


**Figure 1.** Gibbs free energy profile ( $\Delta G$ , in kcal mol<sup>-1</sup>) of the 32CA reaction between nitron 7 and BCP 10.

The geometries of the TSs involved in the 32CA reaction between nitron 7 and BCP 10 are given in Figure 2. The lengths of the C-C and O-C forming bonds at the TSs are 2.132 and 2.211 Å at **TS-10-on**, 2.123 and 2.254 Å at **TS-10-ox**, 2.308 and 1.932 Å at **TS-10-mn** and 2.429 and 1.918 Å at **TS-10-mx**. The O-C bond in the TSs associated with the most favourable *meta* channels is shorter than the C-C one. However, for the *ortho* channel, the C-C bond is slightly shorter than the O-C one. These geometric parameters suggest an

asynchronous bond formation process along the most favourable *meta* regioisomeric channel but an almost synchronous one along the *ortho* reactive channel.

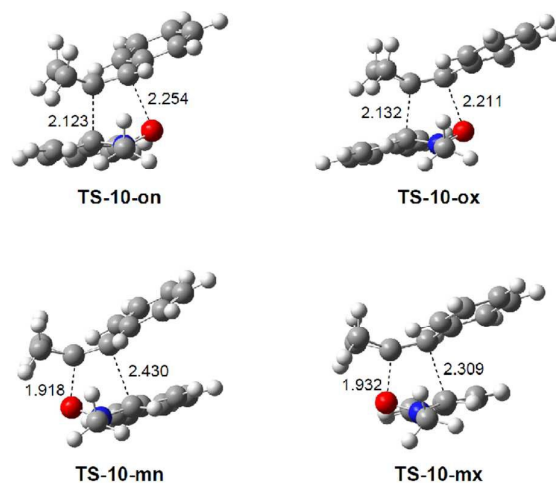


**Figure 2.** MPWB1K/6-31G(d) optimised structures of the TSs of the 32CA reaction of nitrone **7** with BCP **10**. Lengths are given in Angstroms.

The evaluation of the global electron-density transfer (GEDT) along these 32CA reactions is made by a Natural Population Analysis (NPA).<sup>30</sup> The MPWB1K/6-31G(d) natural atomic charges at the TSs were shared between nitrone **7** and BCP **10**. The values of the GEDT at the TSs, which fluxes from BCP **10** toward nitrone **7**, are 0.04e at **TS-10-on**, 0.05e at **TS-10-ox**, 0.06e at **TS-10-mn** and 0.05e at **TS-10-mx**. These very low values indicate that this 32CA reaction has a non-polar character, thus explaining the high activation energy found in this *zw*-type 32CA reaction.<sup>9</sup>

### 3.2 Study of the 32CA reaction between nitrone **7** and BCPC **8**

Next, the 32CA reaction of nitrone **7** with BCPC **8** was studied (see Scheme 4). Total and relative energies for the stationary points (reactants, TSs and cycloadducts) involved in the 32CA reactions of nitrone **7** with BCPC **8**, in gas phase and in toluene, are displayed in Table 3. The IRCs from the four isomeric TSs to the separated reagents end in a series of molecular complexes (MCs) formed in an earlier stage of the reaction in which nitrone **7** and BCPC **8** are positioned in a parallel disposition at a distance of *ca* 3.3 Å. Only the most favorable **MC-8-on** among the four isomeric MCs, which is 7.3 kcal mol<sup>-1</sup> more stable than the separates reagents, was studied (see later). The gas phase activation energies associated with the four reactive channels of this 32CA reaction are 12.0 (**TS-8-on**), 18.1 (**TS-8-ox**),

14.7 (**TS-8-mn**) and 15.4 (**TS-8-mx**) kcal mol<sup>-1</sup>, the reaction being exothermic by 37.2 (**9-on**), 40.9 (**9-ox**), 38.1 (**9-mn**) and 39.6 (**9-mx**) kcal mol<sup>-1</sup>. The activation energy associated with the most favourable *ortho/endo* pathway of this 32CA reaction, 12.0 kcal mol<sup>-1</sup> (**TS-8-on**), is only 2.4 kcal mol<sup>-1</sup> lower than that associated with the most favourable *meta/endo* pathway of the 32CA reaction with BCP **10**, this *zw-type* 32CA being also unfavourable. These energy results indicate that the 32CA reaction between nitrene **7** and BCPC **8** is highly *ortho* regioselective as the most favourable *ortho* **TS-8-on** is 2.7 kcal mol<sup>-1</sup> below *meta* **TS-8-mx**, and displays high *endo* stereoselectivity as the most favourable *endo* **TS-8-on** is 3.4 kcal mol<sup>-1</sup> below *exo* **TS-8-mx**, in good agreement with the experimental observations. These energy values clearly indicate that the presence of the CO<sub>2</sub>Me groups in the cyclopropane ring of BCPC **8** favours the *ortho/endo* pathway, decreasing the corresponding activation energy from 16.4 (**TS-10-on**) in the 32CA reaction between nitrene **7** and BCP **10** to 12.0 kcal mol<sup>-1</sup> in the 32CA reaction of nitrene **7** with BCPC **8**. The high exothermic character of this 32CA reaction makes the cycloaddition irreversible.

**Table 3.** MPWB1K/6-31G(d) total (E, in a.u.) and relative<sup>a</sup> ( $\Delta E$ , in kcal mol<sup>-1</sup>) energies, in gas phase and in toluene, of the stationary points involved in the 32CA reaction of nitrene **7** with BCPC **8**.

	<i>Gas phase</i>		<i>Toluene</i>	
	E	$\Delta E$	E	$\Delta E$
<b>7</b>	-439.94778		-439.95239	
<b>8</b>	-842.37274		-842.37827	
<b>MC-8-on</b>	-1282.33217	-7.31	-1282.33957	-5.6
<b>TS-8-on</b>	-1282.30146	12.0	-1282.30824	14.1
<b>TS-8-ox</b>	-1282.29169	18.1	-1282.29885	20.0
<b>TS-8-mn</b>	-1282.29716	14.7	-1282.30464	16.3
<b>TS-8-mx</b>	-1282.29604	15.4	-1282.30342	17.1
<b>9-on</b>	-1282.37986	-37.2	-1282.38582	-34.6
<b>9-ox</b>	-1282.38565	-40.9	-1282.39132	-38.1
<b>9-mn</b>	-1282.38122	-38.1	-1282.38830	-36.2
<b>9-mx</b>	-1282.38681	-41.6	-1282.39306	-39.6

<sup>a</sup>Relative to **7** and **8**.

Single point energy calculations at the MPWB1K/6-31+G(d) level increases the activation energies by *ca.* 3 kcal mol<sup>-1</sup> and decreases the exothermicities between 4 and 5 kcal mol<sup>-1</sup> as a consequence of a higher stabilisation of reagents than TSs and cycloadducts (see

Table S2 in Supplementary Material). However, inclusion of diffuse functions does not modify the selectivities.

Just as in the 32CA reaction of nitrene **7** with BCP **10**, the inclusion of solvent effects of toluene increases the gas phase activation energies by 2.1 (**TS-8-on**), 1.9 (**TS-8-ox**), 1.6 (**TS-8-mn**) and 1.7 (**TS-8-mx**) kcal mol<sup>-1</sup>. Moreover, solvent effects slightly decrease the exothermic character of the reaction; the changes are 2.6 (**9-on**), 2.8 (**9-ox**), 1.9 (**9-mn**) and 2.0 (**9-mx**) kcal mol<sup>-1</sup>. In spite of the increase of the activation energy and the decrease of the exothermic character, the solvent effect does not modify the selectivity found in gas phase.

The values of the enthalpies, entropies and Gibbs free energies and the relative ones associated with the four reactive channels belonging to the 32CA reaction between nitrene **7** and BCPC **8** are summarized in Table 4. The Gibbs free energy profile of the 32CA reaction between nitrene **7** and BCPC **8** is given in Figure 3. Analysis of the activation enthalpy shows a preference for the *ortho/endo* pathway ( $\Delta H = 14.8$  kcal mol<sup>-1</sup>), in agreement with the computed activation energy. Addition of the entropic contribution increases the activation Gibbs free energy corresponding to the *ortho/endo* pathway to 34.2 kcal mol<sup>-1</sup> favouring kinetically the formation of **9-on** as the single cycloadduct, in good agreement with the experimental outcomes. Note that while formation of **MC-8-on** is exothermic by 4.0 kcal mol<sup>-1</sup>, it is endergonic by 18.3 kcal mol<sup>-1</sup>; consequently, in the Gibbs free energy surfaces these MCs are not a minimum between the reagents and the corresponding TSs.

**Table 4.** MPWB1K/6-31G(d) enthalpies (H, in a.u.), entropies (S, in cal mol<sup>-1</sup> K<sup>-1</sup>) and Gibbs free energies (G, in a.u.), and the relative<sup>a</sup> ones ( $\Delta H$  in kcal mol<sup>-1</sup>,  $\Delta S$  in cal mol<sup>-1</sup> K<sup>-1</sup> and  $\Delta G$  in kcal mol<sup>-1</sup>, respectively), computed at 398.15 K and 1 atm in toluene, for the stationary points involved in the 32CA reaction between nitrene **7** and BCPC **8**.

System	H	$\Delta H$	S	$\Delta S$	G	$\Delta G$
<b>7</b>	-439.78289		102.7		-439.84557	
<b>8</b>	-842.09831		160.1		-842.19609	
<b>MC-8-on</b>	-1281.88765	-4.0	204.3	-58.4	-1282.01242	18.3
<b>TS-8-on</b>	-1281.85764	14.8	212.0	-50.8	-1281.98708	34.2
<b>TS-8-ox</b>	-1281.85004	19.6	204.2	-58.6	-1281.97471	42.0
<b>TS-8-mn</b>	-1281.85426	16.9	206.7	-56.1	-1281.98049	38.4
<b>TS-8-mx</b>	-1281.85317	17.6	212.3	-50.5	-1281.98282	36.9
<b>9-on</b>	-1281.93941	-36.5	199.7	-63.1	-1282.06134	-12.4
<b>9-ox</b>	-1281.93314	-32.6	201.8	-61.0	-1282.05638	-9.2
<b>9-mn</b>	-1281.93487	-33.7	199.4	-63.5	-1282.05662	-9.4
<b>9-mx</b>	-1281.93417	-33.2	199.9	-62.9	-1282.05624	-9.2

<sup>a</sup> Relative to **7** and **8**.

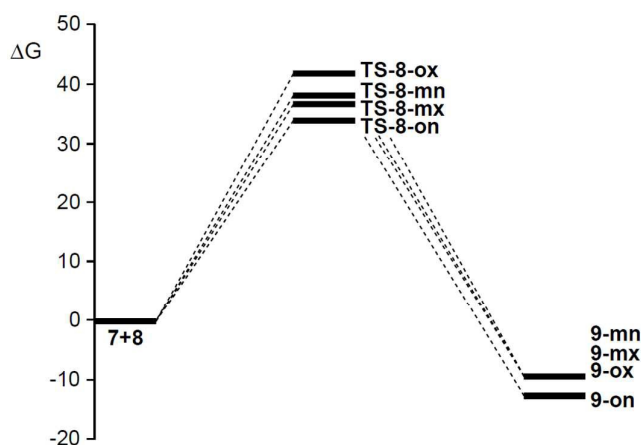


**Figure 3.** Gibbs free energy profile ( $\Delta G$ , in kcal mol<sup>-1</sup>) of the 32CA reaction between nitrone **7** and BCPC **8**.

The geometries of the TSs associated with the 32CA reaction of nitrone **7** with BCPC **8** are given in Figure 4. The lengths of the C–C and O–C forming bonds at the TSs are 2.236 and 2.122 Å at **TS-8-on**, 2.215 and 2.144 Å at **TS-8-ox**, 2.426 and 1.917 Å at **TS-8-mn**, 2.270 and 1.967 Å at **TS-8-mx**.

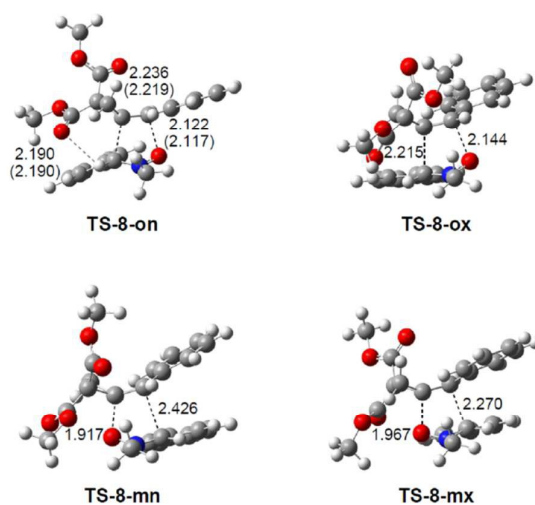


**Figure 4.** MPWB1K/6-31G(d) optimised structures of the TSs of the 32CA reaction of nitrone **7** with BCPC **8**. Lengths are given in Angstroms. The MPWB1K/6-31+G(d) distances are shown in parenthesis.

An analysis of the geometry of **MC-8-on** (see Figure 5) indicates that the carbonyl oxygen atom of one of the two carboxylate groups present in the cyclopropane moiety of BCPC **8** is located at a distance of 2.37 Å from the nitrone C3–H hydrogen atom, which is shortened to 2.19 Å at **TS-8-on**. This geometric arrangement accounts for the large stabilization of **MC-8-on** through the formation of a non-classical hydrogen-bond (HB) in an earlier stage of the reaction. An analysis of the geometry of the MPWB1K/6-31+G(d) optimised **TS-8-on** indicates that the inclusion of diffuse functions does not modify the non-classical CH···O HB (see Figure 4).

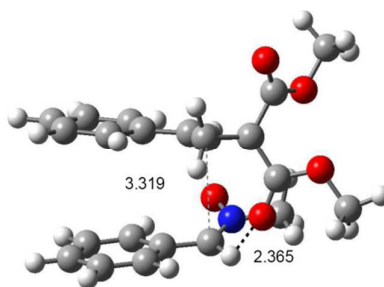


**Figure 5.** Optimised structure of **MC-8-on**. Lengths are given in Angstroms.

Bond order (BO) values have been used to analyse the extent in the bond formation at the TSs. Thus, MPWB1K/6-31G(d) Wiberg bond indices<sup>31</sup> were computed using the NBO method. The BO values for the C–C and O–C forming bonds at the TS associated with this 32CA reaction are 0.29 and 0.29 at **TS-8-on**, 0.32 and 0.28 at **TS-8-ox**, 0.24 and 0.38 at **TS-8-mn** and 0.30 and 0.37 at **TS-8-mx**. These values suggest that the bond formation process at the *meta* TSs is slightly more asynchronous than at the *ortho* TSs, in which the formation of the O–C bond is slightly more advanced than that of the C–C one. Note that at the most favorable **TS-8-on**, analysis of the C–C and O–C BO values indicates a synchronous bond formation process.

The values of the GEDT, which takes place from nitrone **7** to BCPC **8**, are 0.08e (**TS-8-on**), 0.09e (**TS-8-ox**), 0.12e (**TS-8-mn**) and 0.08e (**TS-8-mx**). These very low values indicate

that this *zw-type* 32CA reaction has a non-polar character, in agreement with the obtained high activation energies.<sup>9</sup>

### 3.3 ELF topological analysis along the formation of the C-C and O-C single bonds associated with the most favourable *ortho/endo* reactive channel of the 32CA reaction of nitrene **7** with BCPC **8**

Several theoretical studies have shown that the ELF topological analysis of the changes of electron-density along a reaction path can be used as a valuable tool to understand the bonding changes along the reaction path, and consequently to establish the molecular mechanisms.<sup>32</sup> After an analysis of the electron-density, the ELF provides basins, which are the domains in which the probability of finding an electron pair is maximal.<sup>33</sup> The basins are classified as core basins and valence basins. The latter are characterised by the synaptic order, i.e., the number of atomic valence shells in which they participate. Thus, there are monosynaptic, disynaptic, trisynaptic basins and so on.<sup>34</sup> Monosynaptic basins, labelled V(A), correspond to lone pairs or non-bonding regions, while disynaptic basins, labelled V(A,B), connect the core of two nuclei A and B and, thus, correspond to a bonding region between A and B. This description recovers the Lewis bonding model, providing a very suggestive graphical representation of the molecular system.

Very recently, Ríos-Gutiérrez *et al.* performed a Bonding Evolution Theory (BET) study of the mechanism of 32CA reactions of nitrenes with electron-deficient (ED) ethylenes.<sup>35</sup> Interestingly, this BET study showed that while the formation of the C-C single bond begins at *ca.* 2.0 Å, the formation of the O-C bond begins at the very short distance of 1.6 Å. This study emphasized that the asynchronicity based on the topological analysis of the bonding changes along the reaction is contrary to that obtained by the analysis of the geometrical parameters or the BO values, which predict a more synchronous process.

Herein, in order to understand the formation of the C-C and O-C single bonds along the most favourable *ortho/endo* reactive channel associated with the 32CA reaction of nitrene **7** with BCPC **8**, and thus to establish the molecular mechanism of this 32CA reaction, an ELF topological analysis of the MPWB1K/6-31G(d) wavefunctions of the most relevant points involved in the formation of the C-C and O-C single bonds along the IRC associated with **TS-8-on** has been performed. The population of the most significant valence basins of the

corresponding points is displayed in Table 5, while the attractor positions of the valence basins of the aforementioned points are presented in Figure 6.

The ELF picture of **MC-8-on**,  $d(\text{C3-C4}) = 3.588 \text{ \AA}$  and  $d(\text{O1-C5}) = 3.257 \text{ \AA}$  (see Scheme 4 for atom numbering), which is a minimum in the PES connecting **TS-8-on** with the separated reagents, nitrone **7** and BCPC **8**, recovers the topological characteristics of the separated reagents. The ELF analysis of **MC-8-on** shows two monosynaptic basins,  $V(\text{O1})$  and  $V'(\text{O1})$ , with a population of 2.89e and 3.14e, as well as two disynaptic basins,  $V(\text{O1,N2})$  and  $V(\text{N2,C3})$ , with a population of 1.41e and 3.85e, associated with the oxygen O1 lone pairs and the O1-N2 single and N2=C3 double bond regions of the nitrone framework, respectively. The low electron-density found for the  $V(\text{O1,N2})$  disynaptic basin together with the high population of the  $V(\text{O1})$  and  $V'(\text{O1})$  monosynaptic basins point out a significant polarisation of the O1-N2 single bond towards the oxygen O1 atom. In addition, the ELF topology of **MC-8-on** also shows two disynaptic basins,  $V(\text{C4,C5})$  and  $V'(\text{C4,C5})$ , integrating 1.81e and 1.87e, which belong to the C4=C5 double bond region of the ethylene framework. At **MC-8-on**, there is no GEDT.

At the most favourable *ortho/endo* TS involved in the 32CA between nitrone **7** and BCPC **8**, **TS-8-on**,  $d(\text{C3-C4}) = 2.236 \text{ \AA}$  and  $d(\text{O1-C5}) = 2.122 \text{ \AA}$ , the O1-N2 and N2-C3 bonding regions remain characterised by two  $V(\text{O1,N2})$  and  $V(\text{N2,C3})$  disynaptic basins whose populations has experienced a depopulation to 1.27e and 2.85e, while the C4=C5 double bond of BCPC **8** has strongly been depopulated, being now characterised by the presence of one  $V(\text{C4,C5})$  disynaptic basin integrating 2.84e. The most relevant feature of this TS is the presence of one  $V(\text{C4})$  monosynaptic basin, integrating 0.80e, and one  $V(\text{N2})$  monosynaptic basin, with a population of 1.23e, which is related to the nitrogen N2 lone pair present in isoxazolidine **9-on**. Note that the C4 carbon of BCPC **8** is the most electrophilic center of this molecule (see later). While the electron population of the  $V(\text{C4})$  monosynaptic basin at this TS comes from the strong depopulation of the C4=C5 double bond region of BCPC **8**, the creation of the  $V(\text{N2})$  monosynaptic basin proceeds mainly from the depopulation of the N2=C3 double bond region of nitrone **7** and, in a lesser extent, from the lost electron-density of the  $V(\text{O1,N2})$  disynaptic basin. At this TS, the GEDT presents a very low value, 0.08e, emphasising the non-polar character of this *zw-type* 32CA reaction.

At **P1**,  $d(\text{C3-C4}) = 2.020 \text{ \AA}$  and  $d(\text{O1-C5}) = 1.971 \text{ \AA}$ , two relevant topological changes associated with the formation of the C3-C4 and O1-C5 single bonds are observed: a new  $V(\text{C3})$  monosynaptic basin integrating 0.45e is created together with a new  $V(\text{C5})$

monosynaptic basin integrating 0.18e. The population of these monosynaptic basins comes from the depopulation of the V(N2,C3) and V(C4,C5) disynaptic basins to 2.24e and 2.45e, respectively. Together with the creation of the new V(C5) monosynaptic basin, the total population of the V(O1) and V'(O1) monosynaptic basins has decreased to 5.86e. At the same time, the populations of the V(C4) monosynaptic basin and the V(N2) monosynaptic basin present at **TS-8-on** have increased to 1.03e and 1.69e. Note that the two V(C3) and V(C4) monosynaptic basins are demanded for the formation of the first C3–C4 single bond. At this point, GEDT is again almost negligible, 0.01e.

At **P2**,  $d(\text{C3-C4}) = 1.947 \text{ \AA}$  and  $d(\text{O1-C5}) = 1.915 \text{ \AA}$ , the first most relevant topological change along the IRC is observed. The V(C3) and V(C4) monosynaptic basins present at **P1** are merged into the new V(C3,C4) disynaptic basin, which presents an electron-population of 1.58e (see Figure 6). This topological change indicates that the formation of the C3–C4 single bond has already started at a length of 1.95 Å through the C-to-C coupling of the two C3 and C4 *pseudoradical centers* present at **P1**.<sup>30</sup> Meanwhile, the population of the V(C5) monosynaptic basin slightly increases to 0.22e simultaneously with the decrease of the population of the V(C4,C5) disynaptic basin by 0.10e, and the population of the V(O1,N2) and V(N2,C3) disynaptic basins continue decreasing, contributing to the increase of the electron-density gathered at the nitrogen N2 atom to 1.84e, which can be almost considered a lone pair. The total population of the V(O1) and V'(O1) monosynaptic basins remains practically unchanged. At **P2**, there is a slight change in the flux direction of the GEDT, – 0.02e.

At **P3**,  $d(\text{C3-C4}) = 1.447 \text{ \AA}$  and  $d(\text{O1-C5}) = 1.731 \text{ \AA}$ , the most notable topological change is the disappearance of the V(C5) monosynaptic basin present at the previous **P2**. Interestingly, this disappearance is accompanied by a significant increase of the total population of the V(O1) and V'(O1) monosynaptic basins by 0.33e to reach a higher population than that found at **P1**. The electron-population lost by the V(O1,N2) and V(N2,C3) disynaptic basins since reaching 1.01e and 2.00e is completely collected at the nitrogen N2 atom, the population of the V(N2) monosynaptic basin being increased by 0.29e. This fact suggests that there is a relation between the V(C5) monosynaptic basin present at **P1** and **P2** and the oxygen O1 lone pairs. It can also be observed that the N2–C3 bonding region has already acquired single bond character. In addition, the V(C3,C4) disynaptic basin appeared at the previous **P2** has increased its population to 1.78e as the consequence of the depopulation of the V(C4,C5) disynaptic basin to 2.19e, which indicates that the C4–C5 bond can be

already considered as a single bond too. The GEDT that now fluxes from the ethylene framework towards the nitron one moderately increases until reaching the value of 0.14e.

At **P4**,  $d(\text{C3-C4}) = 1.727 \text{ \AA}$  and  $d(\text{O1-C5}) = 1.709 \text{ \AA}$ , the second most relevant change along the reaction path is observed. A new  $V(\text{O1,C5})$  disynaptic basin appears with a population of 0.73e (see Figure 6) at the same time that the  $V(\text{O1})$  and  $V'(\text{O1})$  monosynaptic basins are strongly depopulated by 0.70e to reach 5.52e. This topological change indicates that the formation of the second O1-C5 single bond has already begun at a length of 1.71 Å through the donation of some electron-density of the oxygen O1 lone pairs of the nitron framework to the C5 carbon of the ethylene moiety. The electron-population of the other basins scarcely varies. The GEDT remains almost unchanged.

Finally, at isoxazolidine **9-on**,  $d(\text{C3-C4}) = 1.534 \text{ \AA}$  and  $d(\text{O1-C5}) = 1.420 \text{ \AA}$ , it is noteworthy that the O1-C5 and O1-N2 single bonds are very polarised toward the oxygen atom, the population of the  $V(\text{O1,C5})$  and  $V(\text{O1,N2})$  disynaptic basins and that of the  $V(\text{O1})$  and  $V'(\text{O1})$  monosynaptic basins integrating 1.31e and 0.98e, and 2.51e and 2.60e, respectively. The nitrogen N2 lone pair and the  $V(\text{C3,C4})$  disynaptic basin have increased their populations to 2.37e and 1.85e, while the C4-C5 single bond presents an electron-population of 2.02e. At isoxazolidine **9-on**, the GEDT has reached a large negative value, -0.23e, as a consequence of the strong polarisation of the O1-C5 single bond.

Some appealing conclusions can be drawn from the ELF topological analysis of the most relevant points involved in the formation of the C3-C4 and O1-C5 single bonds along the IRC associated with the most favourable *ortho/endo* reactive channel of the 32CA reaction between nitron **7** and BCPC **8**: *i*) the formation of the C3-C4 single bond begins at a distance of 1.95 Å following Domingo's recently proposed pattern:<sup>30</sup> *a*) depopulation of the double bond regions; *b*) formation of two non-bonding  $V(\text{C})$  and  $V(\text{C}')$  monosynaptic basins; and *c*) formation of a new  $V(\text{C,C}')$  disynaptic basin through the merger of the electron-density of the aforementioned monosynaptic basins; *ii*) formation of the O1-C5 single bond begins with the creation of a new  $V(\text{O1,C5})$  disynaptic basin at the very short distance of 1.71 Å. The electron-density of this new  $V(\text{O1,C5})$  disynaptic basin mainly proceeds from the electron-density of one  $V(\text{O1})$  monosynaptic basin associated with the lone pairs of the nitron O1 oxygen atom. This pattern for the formation of the O1-C5 single bond is similar to that recently found for the formation of the O-C single bond along the *zw-type* 32CA reaction of nitron **7** with ED acrolein **12**, in which the electron-density of the new O-C single bond comes from the nitron oxygen lone pair;<sup>35</sup> *iii*) the formation of the C3-C4 single bond begins

by a two-center interaction involving the most electrophilic center of BCPC **8**, the C4 carbon; *iv*) while the analysis of the bond lengths of the two C3–C4 and O1–C5 forming bonds along the IRC suggests a synchronous bond formation process, the ELF topological analysis of the bond formation along the reaction path suggests a non-concerted *two-stage one-step* mechanism,<sup>36</sup> in which the formation of the second O1–O5 single bond begins once the first C3–C4 is practically formed. Similarly, the BO values of the C3–C4 and O1–C5 forming bonds at **TS-8-on**, 0.29 and 0.29, respectively, suggest a synchronous bond formation process. Consequently, while the BO values in the range from 1.0 to 3.0 can be used as a measure of the bonding electron-density between two neighbouring atoms, BO values in the range from 0.0 to 1.0 cannot provide any information about the bonding evolution along the reaction coordinate;<sup>35</sup> and finally, *v*) the most favourable *ortho* regioisomeric channel of the non-polar 32CA reaction of nitrene **7** with BCPC **8** shows a great similarity along the formation of the C–C and O–C single bonds with that observed in the unfavourable *ortho* regioisomeric channel of the *zw-type* 32CA reaction of nitrene **7** with acrolein **12**.<sup>35</sup> This fact indicates a similar mechanism for the formation of the C–C and O–C single bonds along the *ortho* regioisomeric channels of 32CA reactions of nitrenes with ED ethylenes, supporting the general model for the bonding changes along the two regioisomeric channels associated with these important reactions.<sup>35</sup>

**Table 5.** Valence basin populations  $N$  calculated from the ELF at some selected points of the most favourable *ortho/endo* reactive channel associated with the 32CA reaction of nitrene **7** with BCPC **8**. Lengths are given in Angstroms. The GEDT obtained by NBO analysis is given in e.

	MC-8-on	TS-8-on	P1	P2	P3	P4	9-on
d(C3–C4)	3.588	2.236	2.020	1.947	1.747	1.727	1.534
d(O1–C5)	3.257	2.122	1.971	1.915	1.731	1.709	1.420
GEDT	0.00	0.08	0.01	-0.02	-0.14	-0.15	-0.23
V(O1,N2)	1.41	1.27	1.21	1.17	1.01	1.00	0.98
V(N2,C3)	3.85	2.85	2.24	2.13	2.00	1.98	1.85
V(N2)		1.23	1.69	1.84	2.13	2.17	2.37
V(C4,C5)	1.81	2.84	2.45	2.35	2.19	2.16	2.02
V'(C4,C5)	1.87						
V(O1)	2.89	3.00	2.96	2.99	3.42	2.74	2.51
V'(O1)	3.14	3.02	2.90	2.90	2.80	2.78	2.60
V(C5)			0.18	0.22			
V(O1,C5)						0.73	1.31

V(C3)		0.45				
V(C4)	0.80	1.03				
V(C3,C4)			1.58	1.78	1.79	1.93

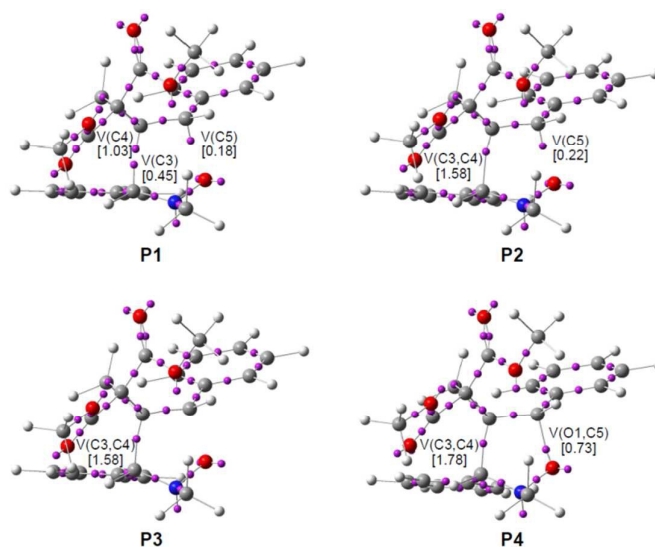


**Figure 6.** ELF attractor positions of the most relevant points associated with the formation of the C3–C4 and O1–C5 single bonds along the most favourable *ortho/endo* regioisomeric channel associated with the 32CA reaction of nitrene **7** with BCPC **8**. The electron-populations, in e, are given in brackets.

### 3.4 NCI analysis of TS-8-on

An analysis of the geometry of **TS-8-on** shows that the carbonyl oxygen atom of one of the two carboxylate groups of BCPC **8** is positioned towards the nitrene C3–H hydrogen atom, with an O–H distance of 2.19 Å. This short distance suggests the formation of a non-classical HB, present also in **MC-8-on**, which could justify the stabilisation of **MC-8-on** and **TS-8-on**. In order to explain the stabilisation of these species by the formation of a HB between the carbonyl oxygen atom and the nitrene hydrogen atom, an NCI analysis,<sup>22</sup> was performed. Figure 7 represents the reduced density gradient for **MC-8-on** and **TS-8-on**, while Figure 8 displays low-gradient isosurfaces, subject to the constraint of low density, for these species.

NCIs have a unique signature and their presence can be revealed solely by means of the electron-density analysis. They are highly non-local and manifest in real space as low-gradient isosurfaces with low densities. The sign of the Laplacian of the density,  $\nabla^2 \rho$ , is a

widely used tool to distinguish between different types of strong interactions.<sup>37</sup> To analyse bonding in more detail, the Laplacian is often decomposed into a sum of contributions. These components are the three eigenvalues  $\lambda_i$  of the electron-density Hessian matrix, such that  $\nabla^2\rho = \lambda_1 + \lambda_2 + \lambda_3$ . Analysis of these components has been widely applied to chemical bonding. The sign of  $\lambda_2$  can be used to distinguish bonded ( $\lambda_2 < 0$ ) from non-bonded ( $\lambda_2 > 0$ ) interactions. Analysis of the sign of  $\lambda_2$  thus helps to differentiate between different types of NCIs, whereas the density itself provides information about their strength. Therefore, in a representation of the reduced density gradient (RDG) versus electron-density, low-density low-gradient spikes lying at negative values indicate stabilising interactions; low-density low-gradient spikes at positive values indicate the lack of bonding, while if they are near zero they are indicative of weak attractive or repulsive interactions.<sup>22</sup> The locations of these peaks are sensitive to the atom types involved, the interaction strengths and the level of theory used to obtain the density.

On the other hand, the gradient isosurfaces provide a useful visualization of NCIs as broad regions of real space, rather than simple pairwise contacts between atoms, and are coloured according to the corresponding values of  $\text{sign}(\lambda_2)\rho$ . Surfaces with very low density values ( $\rho < |0.005|$  a.u.) generally represent weaker dispersion interactions, while surfaces with slightly higher density values ( $|0.005| < \rho < |0.05|$  a.u.) represent stronger NCIs, including both attractive HBs and steric clashes. Thus, large negative values of  $\text{sign}(\lambda_2)\rho$  are indicative of attractive interactions (such as dipole-dipole or hydrogen bonding) and are coloured in blue, while if  $\text{sign}(\lambda_2)\rho$  is large and positive, the interactions are non-bonding and are coloured in red; values near zero indicate very weak van der Waals interactions, and are coloured in green.

The presence of a turquoise surface between the oxygen and hydrogen atoms in **TS-8-on** in Figure 8b reveals the existence of an HB between them, which is evidenced by the low-density low-gradient turquoise spike at  $-0.022$  a.u. in Figure 7b. The green spikes at *ca.*  $-0.014$  a.u. are indicative of weak van der Waals interactions, while the blue spike appearing at the large negative value of  $-0.056$  a.u. is associated with the strong attractive interactions preceding the bond formation. This is evident from the degree of blue shading for the different interactions in Figure 8b. Note that the blue spike associated with the strong attractive bond formation interactions that take place at **TS-8-on** is obviously not present in the graphic related to **MC-8-on** (see Figures 7b and 7a, respectively), while that associated with the HB is already present, indicating that this non-classical HB is formed at the

beginning of the reaction. Interestingly, the proximity of the spikes associated with the HB and the van der Waals interactions emphasizes the weakness of the former, in agreement with the colour surface itself, but it is significant enough to change the predicted regioselectivity (see later).

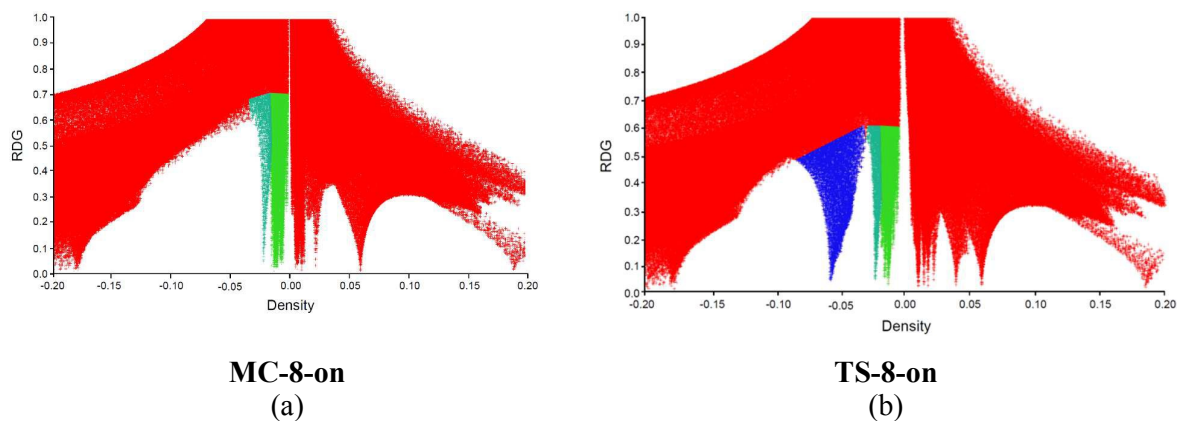


**Figure 7.** Plots of the RDG versus the electron-density multiplied by the sign of the second Hessian eigenvalue for (a) **MC-8-on** and (b) **TS-8-on**. Both quantities are given in a.u.

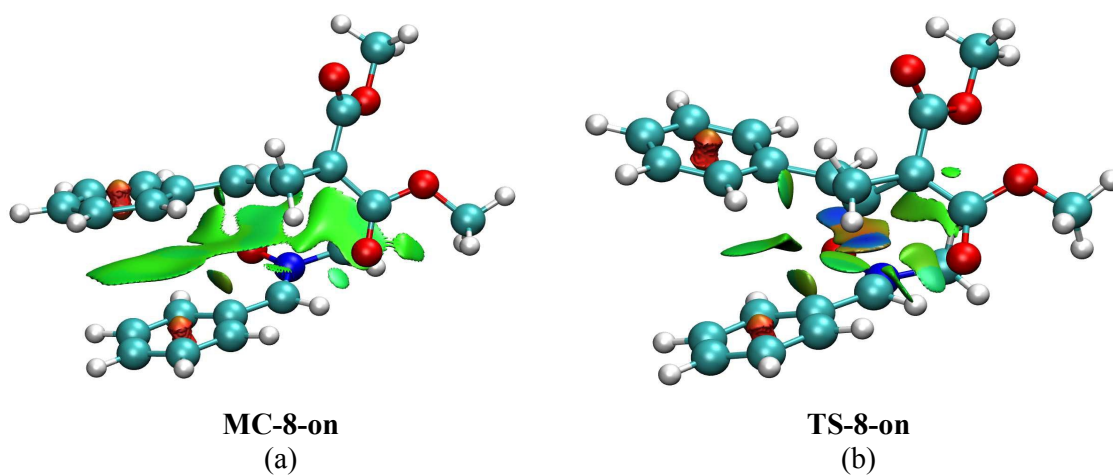


**Figure 8.** NCI gradient isosurfaces of (a) **MC-8-on** and (b) **TS-8-on**. Blue indicates strong attractive interactions while red indicates strong non-bonded overlap.

Finally, NCIs analysis of the MPWB1K/6-31+G(d) optimised **TS-8-on** indicates that the inclusion of diffuse functions does not modify the non-classical CH...O HB found at the MPWB1K/6-31G(d) level (see Figures S1 and S2 in Supplementary Material).

### 3.5 DFT-based reactivity indices analysis

The nature of the mechanism of these 32CA reactions has been analysed using the global indices, as defined in the context of DFT,<sup>38</sup> which are useful tools to understand the reactivity of molecules in their ground state as shown in recent studies devoted to Diels–Alder and 32CA reactions.<sup>39,40</sup> Table 6 collects the static global properties: electronic chemical potential,  $\mu$ , chemical hardness,  $\eta$ , and global electrophilicity,  $\omega$ , and nucleophilicity,  $N$ , of nitrone **7**, BCPC **8** and BCP **10**.

**Table 6.** MPWB1K/6-31G(d) electronic chemical potential ( $\mu$ ), chemical hardness ( $\eta$ ), global electrophilicity ( $\omega$ ) and global nucleophilicity ( $N$ ), in eV, of nitrone **7** and BCPC **8** and BCP **10**.

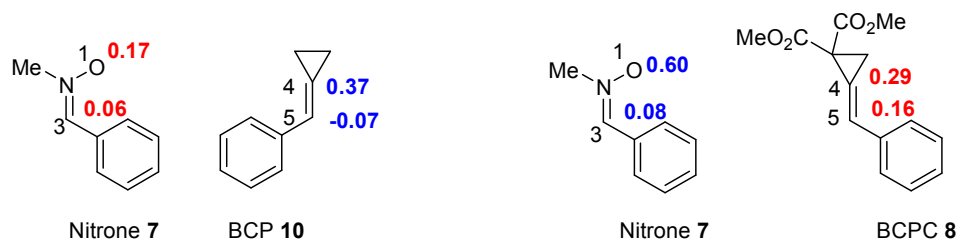
	$\mu$	$\eta$	$\omega$	$N$
BCPC <b>8</b>	-3.62	6.73	0.97	3.24
Nitron <b>7</b>	-3.41	6.09	0.96	3.77
BCP <b>10</b>	-3.29	6.84	0.79	3.52

The electronic chemical potential of nitrone **7**,  $\mu = -3.42$  eV, is similar to that of BCPC **8**,  $\mu = -3.29$  eV and BCP **10**,  $\mu = -3.62$  eV. Thereby, a very low GEDT will be expected along the reactions, suggesting a non-polar mechanism for these 32CA reactions.

The electrophilicity and nucleophilicity indices of nitrone **7**,  $\omega = 0.96$  and  $N = 3.77$  eV, allow its classification as a moderate electrophile and a strong nucleophile based on the electrophilicity<sup>39</sup> and nucleophilicity<sup>41</sup> scales. On the other hand, the electrophilicity and nucleophilicity indices of BCP **10** are  $\omega = 0.79$  and  $N = 3.52$  eV, being classified on the borderline of marginal electrophiles and as a strong nucleophile. Therefore, it is expected that nitrone **7** and BCP **10** participate only as good nucleophiles in polar reactions. Consequently, this reaction will present a high activation energy and proceeds *via* a non-polar mechanism, as indicated by the previous GEDT analysis. The electrophilicity index of BCPC **8** is  $\omega = 0.97$  eV, being classified on the borderline of moderate electrophiles. In spite of the electrophilic activation of BCPC **8** with respect to BCP **10**, the former is not electrophilic enough to

participate in polar reactions. The higher electrophilic character of BCPC **8** than that of nitrone **7** together with the stronger nucleophilic character of the latter indicates that in this 32CA reaction the low flux of electron-density will go from nitrone **7** to BCPC **8**, while in the 32CA reaction of nitrone **7** with BCP **10** there is an inversion in the direction of the GEDT, fluxing from BCP **10** to nitrone **7**.

In polar cycloaddition reactions the most favourable reactive channel is that involving the initial two-center interaction between the most electrophilic and nucleophilic centers of both reagents. Recently, Domingo *et al.*<sup>28</sup> proposed the electrophilic  $P_k^+$  and nucleophilic  $P_k^-$  Parr functions derived from the changes of spin electron-density reached *via* the GEDT process from the nucleophile to the electrophile as powerful tools in the study of the local reactivity in polar processes. Accordingly, the electrophilic  $P_k^+$  Parr functions for nitrone **7** and BCPC **8**, and the nucleophilic  $P_k^-$  Parr functions for nitrone **7** and BCP **10** are analysed in order to predict the most favourable electrophile/nucleophile two-center interaction in these 32CA reactions and, therefore, to explain the regioselectivity experimentally observed.



**Scheme 5.** Electrophilic Parr functions for nitrone **7** and BCPC **8**, in red, and nucleophilic Parr functions for nitrone **7** and BCP **10**, in blue.

For the reaction between nitrone **7** and BCP **10**, analysis of the nucleophilic  $P_k^-$  Parr functions of BCP **10** indicates that the C4 carbon atom is the most nucleophilic center of the molecule,  $P_k^- = 0.37$ . On the other hand, analysis of the electrophilic  $P_k^+$  Parr functions of nitrone **7** indicates that the O1 oxygen is the most electrophilic center of the nitrone framework,  $P_k^+ = 0.17$ . Consequently, the most favourable nucleophilic/electrophilic two-center interaction along an asynchronous single bond formation will take place between the C4 carbon of BCP **10** and the O1 atom of nitrone **7**, leading to the formation of the *meta* regioisomers, in clear agreement with the TSs analysis.

Similarly, for the reaction between nitrone **7** and BCPC **8**, analysis of the electrophilic  $P_k^+$  Parr functions at BCPC **8** indicates that the C4 carbon atom is the most electrophilic center,  $P_k^+ = 0.29$ . On the other hand, analysis of the nucleophilic  $P_k^-$  Parr functions of nitrone **7**

reveals that the O1 oxygen is the most nucleophilic center  $r_k = 0.60$ . Thereby, the most favourable interaction will occur between the O1 oxygen of nitrone **7** and the C4 carbon of BCPC **8** leading to the formation of the *meta* regioisomers, in disagreement with the energies analysis and experimental data.

### 3.6 What is the origin of the *ortho/endo* selectivity?

A comparative analysis of the activation energies associated with the 32CA reactions of nitrone **7** with BCP **10** and BCPC **8** reveals that the main energy change caused by the inclusion of the carboxylate groups in the cyclopropane moiety is the stabilisation of **TS-8-on** by  $4.4 \text{ kcal mol}^{-1}$  with respect to **TS-10-on**, while the other three TSs remain practically unchanged. Consequently, the presence of the carboxylate groups appears to have a significant effect only along the *ortho/endo* reactive channel.

Both, geometrical analysis and NCI topological analysis of the electron-density of **TS-8-on** evidence the presence of a non-classical HB interaction between the carbonyl oxygen atom of one of the two carboxylate groups of BCPC **8** and the nitrone C3-H hydrogen atom. Due to the low regioselectivity found in the non-polar 32CA reaction between nitrone **7** and BCP **10**,  $\Delta\Delta H^\ddagger = 0.6 \text{ kcal mol}^{-1}$ , formation of this HB in **TS-8-on**, which can be estimated to be *ca.*  $7 \text{ kcal mol}^{-1}$ , overcomes this low energy and changes the regioselectivity predicted by the Parr functions. Interestingly, the proximity of the spikes associated with the HB and the van der Waals interactions emphasizes the weakness of the former, in agreement with the colour surface itself (see above), but it is significant enough to change the regioselectivity. Note that the *exo* stereoselective channels associated with the 32CA reaction between nitrone **7** and BCPC **8** remain *meta* regioselective, since **TS-8-mx** is  $2.7 \text{ kcal mol}^{-1}$  below **TS-8-ox**.

## 4. Conclusions

The role of the CO<sub>2</sub>Me groups in the reactivity, selectivity and mechanism in the 32CA reactions of *C*-phenyl-*N*-methylnitronone **7** with BCPC **8** has been investigated using DFT methods at the MPWB1K/6-31G(d) level. To this end, a comparative study of the molecular mechanism and the regio- and stereoselectivities for the 32CA reactions of *C*-phenyl-*N*-methylnitronone **7** with BCPC **8** and BCP **10** has been performed. Four reactive channels associated with the *ortho/meta* regio- and *endo/exo* stereoselective approach modes have been explored and characterised for each reaction. The following conclusions can be drawn from our results:

- i) The 32CA reaction between nitrone **7** and BCP **10** takes place through a one-step mechanism. This 32CA reaction presents low selectivity. The low GEDT found at the corresponding TSs indicates the non-polar character of this *zw-type* 32CA reaction, explaining the high activation energy found in this 32CA reaction. Inclusion of solvent effects slightly increases the activation energy and decreases the exothermic character of the 32CA reactions as a consequence of a larger solvation of reagents than TSs and CAs.
- ii) The 32CA reaction of nitrone **7** with BCPC **8** proceeds *via* a one-step mechanism with a non-polar character leading to the formation of the *ortho/endo* cycloadduct as the kinetic product experimentally observed. Inclusion of solvent effects does not cause any remarkable change in the selectivity obtained in gas phase.
- iii) ELF topological analysis of the most relevant points involved in the formation of the C3–C4 and O1–C5 single bonds along the IRC associated with the most favourable *ortho/endo* reactive channel of the 32CA reaction between nitrone **7** and BCPC **8** indicates that while formation of the C3–C4 single bond begins at a distance of 1.95 by a C-to-C coupling of two *pseudodiradical* centers generated at the C3 and C4 atoms, formation of the O1–C5 single bond begins at the very short distance of 1.71 Å by the electron-density provided by the lone pairs of the nitrone O1 oxygen atom. This model for the formation of the C–C and O–C single bonds is similar to that recently described for the 32CA reactions between nitrones and ED ethylenes.<sup>35</sup>
- iv) While the analysis of the bond lengths of the two C3–C4 and O1–C5 forming bonds along the IRC associated with the most favourable *ortho/endo* reactive channel of the 32CA reaction between nitrone **7** and BCPC **8** suggests a synchronous bond formation process, the ELF topological analysis of the bond formation along the reaction path suggests a non-concerted *two-stage one-step* mechanism<sup>36</sup> in which the formation of the second O1–O5 single bond begins once the first C3–C4 is practically formed. Consequently, it is relevant to emphasize that the analyses of the asynchronicity based on the bond lengths or BO values are not adequate when the formation of C–C and O–C single bonds is involved, a very usual feature in 32CA reactions.
- v) Analysis of the global DFT reactivity indices explains the electronic behaviour of these 32CA reactions. The non-polar character of these *zw-type* 32CA reactions and the high activation energies are the consequence of the poor electrophilic character of the reagents in spite of their strong nucleophilic character.

- vi) Analysis of the Parr functions predicts a *meta* regioselectivity for the 32CA reaction of nitrene **7** with BCPC **8**, which is different than that experimentally observed.
- vii) NCI topological analysis of the electron-density of the most favourable **TS-8-on** suggests the formation of a non-classical HB between the carbonyl oxygen atom of one of the two carboxylate groups of BCPC **8** and the nitrene C3-H hydrogen atom. Formation of this non-classical HB, which provokes a stabilisation of *ca.* 7 kcal mol<sup>-1</sup>, can overcome the low *meta* regioselectivity found in the 32CA reaction of nitrene **7** with BCP **10**, explaining the *ortho/endo* selectivity experimentally found.

### Supporting Information

B3LYP/6-31G(d) gas phase total and relative energies of the stationary points involved in the 32CA reaction of *C*-phenyl-*N*-methylnitrene **7** with BCP **10**. MPWB1K/6-31+G(d)//MPWB1K/6-31G(d) gas phase total and relative energies of the stationary points involved in the 32CA reaction between *C*-phenyl-*N*-methylnitrene **7** with BCPC **8**. Overlaid plots of the RDG versus the electron-density multiplied by the sign of the second Hessian eigenvalue for the MPWB1K/6-31G(d) and MPWB1K/6-31+G(d) optimised geometry of **TS-8-on**, as well as the corresponding NCI gradient isosurfaces and finally, MPWB1K/6-31G(d) gas phase computed total electronic energies and cartesian coordinates of all the stationary points involved in the studied 32CA reactions. The imaginary frequencies of the TSs are also included.

### Acknowledgements

This work has been supported by the Ministerio de Economía y Competitividad of the Spanish Government; project CTQ2013-45646-P. M. R.-G. Thanks the Ministerio de Economía y Competitividad for a pre-doctoral contract co-financed by the European Social Fund (BES-2014-068258).

### References

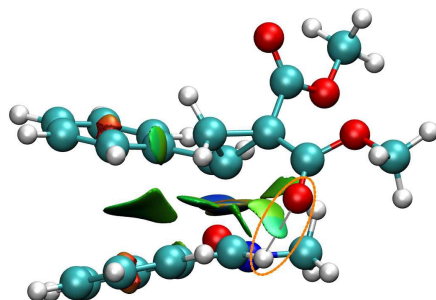
- 1 (a) W. Carruthers, *Some Modern Methods of Organic Synthesis*, 2nd ed.; Cambridge University Press: Cambridge, 1978; (b) W. Carruthers, *Cycloaddition Reactions in Organic Synthesis*; Pergamon: Oxford, 1990; (c) A. Padwa, *Dipolar Cycloaddition*

- Chemistry*; Wiley-Interscience: New York, NY, 1984; Vol. 1; (d) R. Grigg, *Chem. Soc. Rev.*, 1987, **16**, 89.
- 2 (a) K. V. Gothelf and K. A. Jørgensen, *Chem. Rev.*, 1998, **98**, 863; (b) S. Karlsson and H. E. Högberg, *Org. Prep. Proced. Int.*, 2001, **33**, 103; (c) S. Kobayashi and K. A. Jørgensen, *Cycloaddition Reactions in Organic Synthesis*; Wiley-VCH: Weinheim, 2002; (d) H. Pellissier, *Tetrahedron*, 2007, **63**, 3235.
- 3 (a) G. Wess, W. Kramer, G. Schubert, A. Enhsen, K. H. Baringhaus, H. Globmik, S. Müller, K. Bock, H. Klein, M. John, G. Neckermann and A. Hoffmann, *Tetrahedron Lett.*, 1993, **34**, 819; (b) P. Ding, M. Miller, Y. Chen, P. Helquist, A. J. Oliver and O. Wiest, *Org. Lett.*, 2004, **6**, 1805.
- 4 A. Padwa. and W. H. Pearson, *Synthetic Applications of 1,3-Dipolar Cycloaddition Chemistry Toward Heterocycles and Natural Products*; Wiley & Sons: New York, 2002.
- 5 (a) A. Brandi, S. Cicchi, F. M. Cordero and A. Goti, *Chem. Rev.*, 2003, **103**, 1213; (b) A. Brandi and A. Goti, *Chem. Rev.* 1998, **98**, 589; (c) F. M. Cordero, F. De Sarlo and A. Brandi, *Monatsh. Chem.*, 2004, **135**, 649.
- 6 A. K. Nacereddine, W. Yahia, C. Sobhi, A. Djerourou, *Tetrahedron Lett.*, 2012, **53**, 5784.
- 7 F. Moeinpour and A. Khojastehnezhad. *J. Iran. Chem. Soc.*, 2014, **11**, 1459.
- 8 L. R. Domingo and S. R. Emamian, *Tetrahedron*, 2014, **70**, 1267.
- 9 L. R. Domingo, M. J. Aurell, P. Pérez, *Tetrahedron*, 2014, **70**, 4519.
- 10 T. Q. Tran, V. V. Diev and A. P. Molchanov, *Tetrahedron*, 2011, **67**, 2391.
- 11 C. Lee, W. Yang and R. G. Parr, *Phys. Rev. B: Condens. Matter Mater. Phys.*, 1988, **37**, 785; (b) A. D. Becke, *J. Chem. Phys.*, 1993, **98**, 5648.
- 12 (a) C. E. Check, T. M. Gilbert, *J. Org. Chem.*, 2005, **70**, 9828; (b) G. O. Jones, V. A. Guner, K. N. Houk, *J. Phys. Chem. A*, 2006, **110**, 1216; (c) G. A. Griffith, I. H. Hillier, A. C. Moralee, J. M. Percy, R. Roig, M. K. Vicent, *J. Am. Chem. Soc.*, 2006, **128**, 13130.
- 13 Y. Zhao and D. G. Truhlar, *J. Phys. Chem. A*, 2004, **108**, 6908.

- 14 W. J. Hehre, L. Radom, P. v. R. Schleyer and J. A. Pople, *Ab initio Molecular Orbital Theory*; Wiley: New York, 1986.
- 15 K. Fukui, *J. Phys. Chem.*, 1970, **74**, 4161.
- 16 (a) J. Tomasi and M. Persico, *Chem. Rev.*, 1994, **94**, 2027; (b) B. Y. Simkin, I. Sheikhet, *Quantum Chemical and Statistical Theory of Solutions-A Computational Approach* Ellis Horwood: London, 1995.
- 17 Becke. A. D, *J. Chem. Phys.*, 1993, **98**, 5648.
- 18 A. P. Scott and L. Radom. *J. Phys. Chem.*, 1996, **100**, 16502.
- 19 (a) A. E. Reed, R. B. Weinstock and F. Weinhold, *J. Chem. Phys.*, 1985, **83**, 735; (b) A. E. Reed, L. A. Curtiss and F. Weinhold, *Chem. Rev.*, 1988, **88**, 899.
- 20 (a) A. Savin, A. D. Becke, J. Flad, R. Nesper, H. Preuss and H. G. Vonschnering, *Angew. Chem. Int. Ed.*, 1991, **30**, 409; (b) B. Silvi and A. Savin, *Nature*, 1994, **371**, 683; (c) A. Savin, B. Silvi and F. Colonna, *Can. J. Chem.*, 1996, **74**, 1088; (d) A. Savin, R. Nesper, S. Wengert and T. F. Fassler, *Angew. Chem. Int. Ed. Engl.*, 1997, **36**, 1808.
- 21 S. Noury, X. Krokidis, F. Fuster and B. Silvi, *Comput. Chem.*, 1999, **23**, 597.
- 22 E. R. Johnson, S. Keinan, P. Mori-Sanchez, J. Contreras-Garcia, J. Cohen and A. W. Yang, *J. Am. Chem. Soc.*, 2010, **132**, 6498.
- 23 (a) J. R. Lane, J. Contreras-Garcia, J.-P. Piquemal, B. J. Miller and H. G. Kjaergaard, *J. Chem. Theory. Comput.*, 2013, **9**, 3263; (b) J. Contreras-Garcia, E. R. Johnson, S. Keinan, R. Chaudret, J.-P. Piquemal and D. N. Beratan, W. Yang, *J. Chem. Theory. Comput.*, 2011, **7**, 625.
- 24 M. J. Frisch, *et al.*, Gaussian 09, Revision A.02, Gaussian Inc, Wallingford CT, 2009.
- 25 R. G. Parr, L. von Szentpaly and S. Liu, *J. Am. Chem. Soc.*, 1999, **121**, 1922.
- 26 (a) R. G. Parr and R. G. Pearson, *J. Am. Chem. Soc.*, 1983, **105**, 7512; (b) R. G. Parr and W. Yang, *Density Functional Theory of Atoms and Molecules*; Oxford University Press: New York, 1989.
- 27 (a) L. R. Domingo.; E. Chamorro.; P. Pérez, *J. Org. Chem.*, 2008, **73**, 4615; (b) L. R. Domingo.; P. Pérez, *Org. Biomol. Chem.*, 2011, **9**, 7168.
- 28 L. R. Domingo, P. Pérez and J. A. Sáez, *RSC Adv.*, 2013, **3**, 1486.
- 29 W. Benchouk., S. M. Mekelleche, B. Silvi, M. J. Aurell, and L. R. Domingo, *J. Phys. Org. Chem.*, 2011, **24**, 611.
- 30 L. R. Domingo, *RSC Adv.*, 2014, **4**, 32415.
- 31 K. B. Wiberg, *Tetrahedron*, 1968, **24**, 1083.

- 32 (a) S. Berski, J. Andrés, B. Silvi and L. R. Domingo, *J. Phys. Chem. A*, 2003, **107**, 6014; (b) V. Polo, J. Andrés, S. Berski, L. R. Domingo and B. Silvi, *J. Phys. Chem. A*, 2008, **112**, 7128; (c) J. Andrés, P. González-Navarrete and V. S. Safont, *Int. J. Quant. Chem.*, 2014, **114**, 1239; (d) J. Andrés, S. Berski, L. R. Domingo, V. Polo and B. Silvi, *Curr. Org. Chem.*, 2011, **15**, 3566; (e) J. Andrés, L. Gracia, P. González-Navarrete and V. S. Safont, *Comp. Theor. Chem.*, 2015, **1053**, 17.
- 33 A. Savin, *J. Chem. Sci.*, 2005, **117**, 473.
- 34 B. Silvi, *J. Mol. Struct.*, 2002, **614**, 3.
- 35 Mar Ríos-Gutiérrez, P. Pérez and L. R. Domingo, *RSC Adv.*, 2015, **5**, 58464.
- 36 L. R. Domingo, J. A. Saéz, R. J. Zaragozá and M. Arnó *J. Org. Chem.* 2008, **73**, 8791.
- 37 Bader, R. F. W.; Essén, H. *J. Chem. Phys.* 1984, **80**, 1943.
- 38 P. Geerlings, F. De Proft and W. Langenaeker., *Chem. Rev.*, 2003, **103**, 1793; (b) D. H. Ess, G. O. Jones and K. N. Houk., *Adv. Synth. Catal.*, 2006, **348**, 2337.
- 39 L. R. Domingo, M.J. Aurell, P. Pérez and R. Contreras, *Tetrahedron*, 2002, **58**, 4417.
- 40 P. Pérez, L. R. Domingo, M. J. Aurell and R. Contreras, *Tetrahedron*, 2003, **59**, 3117.
- 41 P. Jaramillo, L. R. Domingo, E. Chamorro and P. Pérez, *J. Mol. Struct. (Theochem)*, 2008, **865**, 68.

### Graphical Abstract



NCIs in the *ortho/endo* TS

Formation of a non-classical CH...O hydrogen-bond involving the nitrene C-H hydrogen is responsible for the selectivity experimentally found in this non-polar *zw-type* 32CA reaction.